Int J Thermophys
DOI 10.1007/s10765-007-0208-9

Application of the TraPPE Force Field to Predicting Isothermal Pressure–Volume Curves at High Pressures and High Temperatures

Becky L. Eggimann · J. Ilja Siepmann · Laurence E. Fried

© Springer Science+Business Media, LLC 2007

Abstract Knowledge of the thermophysical properties of materials at extreme pressure and temperature conditions is essential for improving our understanding of many planetary and detonation processes. Significant gaps in what is known about the behavior of materials at high density and high temperature exist, largely, due to the limitations and dangers of performing experiments at the necessary extreme conditions. Modeling these systems through the use of equations of state and particle-based simulation methods significantly extends the range of pressures and temperatures that can be safely studied. The reliability of such calculations depend on the accuracy of the models used. Here we present an assessment of the united-atom version of the TraPPE (transferable potentials for phase equilibria) force field and single-site exp-6 representations for methane, methanol, oxygen, and ammonia at extreme conditions. As shown by Monte Carlo simulations in the isobaric–isothermal ensemble, the TraPPE models, despite being parameterized to the vapor–liquid coexistence curve (i.e., relatively mild conditions), perform remarkably well in the high-pressure/high-temperature regime. The single-site exp-6 models can fit experimental data in the high-pressure/tempera-

B. L. Eggimann · J. I. Siepmann (✉)
Departments of Chemistry and of Chemical Engineering and Materials Science,
University of Minnesota,
207 Pleasant Street SE, Minneapolis, MN 55455-0431, USA
e-mail: siepmann@chem.umn.edu

B. L. Eggimann
Department of Chemistry, Wheaton College,
Wheaton, IL 60187, USA

L. E. Fried (✉)
Chemistry, Materials, and Life Sciences Directorate, Lawrence Livermore National Laboratory,
Livermore, CA 94550, USA
e-mail: lfried@llnl.gov

ture regime very well, but the parameters are less transferable to conditions below the critical temperature.

Keywords Equation of state · Extreme conditions · Monte Carlo simulation · Transferable force field

1 Introduction

Many of the most common elements and molecules in the universe exist in highly compressed environments. The interior of planets and stars account for far more matter than the exterior surfaces, yet comparatively little is known about the thermophysical properties of small molecules under such extreme pressures and temperatures. At the high densities of planetary interiors, molecular properties can be very different from those observed at the ambient conditions of the Earth's surface [1]. A more complete understanding of the thermophysics of systems at high pressures and temperatures has value for a wide range of disciplines, including planetary physics, detonation processes, and materials science [2].

Despite the importance of studying systems at extreme pressures and temperatures, the dangers and challenges of performing experiments under those conditions are well-known and not easily overcome. While modeling via equations of state or particle-based simulations can be a convenient alternative, these methods have significant limitations. The predictions made by using either analytical equations of state or molecular simulations are only as accurate as the underlying models they employ. With poor availability of experimental data, validation of these models can be difficult. Most models currently in use, even those used in this study, have been fitted to only a limited set of experimental data. Models that make use of transferable parameters (i.e., the same parameters are fitted to be accurate at several state points, including those beyond the constraints of the initial parameterization conditions) are one option for supplementing the low levels of experimental data available for high-pressure/high-temperature systems. With transferability as one of its explicit goals, the transferable potentials for phase equilibria (TraPPE) force field has been developed to reproduce vapor–liquid coexistence curves (i.e., temperatures and pressures well below the extreme region) over a wide range of chemical systems and complexities [3–8]. The TraPPE models have been shown to be reasonably accurate for several systems beyond the state points and molecules used in the parameter fitting [9,10].

In the present work, the high-pressure densities and compressibility factors of CH_4, NH_3, O_2, and CH_3OH are computed for the united-atom version of the TraPPE force field and compared with data obtained experimentally and with predictions from an analytical equation of state based on exp-6 models.

2 Methods

2.1 Monte Carlo Simulations

Monte Carlo simulations were performed in the isobaric–isothermal (NpT) ensemble [11] at state points chosen to correspond to those studied by experiment for CH_4, NH_3, O_2, and CH_3OH. In each simulation, the system consisted of 1,000 molecules periodically replicated in a cubic box. Sampling of the resulting phase space was achieved through translations (all systems), rigid-body rotations [12] (all systems other than CH_4 which is modeled with a single interaction site and has no rotational degrees of freedom), configurational-bias moves [4,13] for conformational changes of CH_3OH, and volume exchanges with an external pressure bath [11] using scaled center-of-mass coordinates. For every system, the simulations were equilibrated for at least 20,000 Monte Carlo cycles (where one cycle consists of $N = 1{,}000$ randomly selected moves), and the production periods consisted of at least 80,000 MC cycles. For each of the systems, five independent simulations were run at every state point. The properties and statistical uncertainties are calculated by averaging over these independent runs.

Molecular interactions in the TraPPE-UA force field [3,6,14,15] are described by pairwise-additive Lennard-Jones (LJ) and Coulomb potentials for the nonbonded interactions. Spherical potential truncation at 14 Å and analytical tail corrections [16] are applied to the LJ interactions, and an Ewald sum with parameters set to $\kappa \times L = 5.6$ and $K_{\max} = 5$ is used to compute the electrostatic interactions [16]. Bonded interactions depend on the specific model employed, but generally consist of fixed bond lengths and harmonic bending potentials. For this work, united-atom models were used, meaning that all the atoms in a CH_x group were treated as a single pseudo-atom. Using this methodology, methane consists of a single interaction site placed at the carbon atom of the CH_4 group. Methanol's CH_3 group is also modeled as a pseudo-atom, while oxygen and hydrogen atoms are modeled explicitly. The oxygen and ammonia models include additional charge sites located at the bond center for O_2 and near the nitrogen atom for NH_3, and both are rigid models. The TraPPE-UA models consist of one, three, three, and five interaction sites for CH_4, CH_3OH, O_2, and NH_3, respectively.

Additional simulations in the isobaric–isothermal ensemble were performed for liquid phases at ambient pressure to consider the transferability of the single-site exp-6 and TraPPE models. The only system that is a liquid at standard conditions (298 K and 1 atm) is methanol, and so the CH_3OH simulations were performed at this temperature and pressure. The other systems were simulated at 1 atm with temperatures set to yield a liquid state (i.e., just below their normal boiling points).

2.2 Equation-of-State Predictions using exp-6 Models

A multi-site representation, as used in the TraPPE-UA force field, allows the user to assemble new molecules from existing building blocks without the need for any parameter fitting and is also essential for an accurate treatment of fluid structure and

Table 1 Single-Site exp-6 parameters

Molecule	r (Å)	ϵ/k_B (K)	α
CH_4	4.319	142.5	12.13
NH_3	3.730	251.6	11.96
O_2	3.865	117.7	13.50
CH_3OH	4.114	506.8	13.00

dynamics. For small molecules, however, molecular shape often plays a minor role in the equation of state and transport properties. In this case effective isotropic single-site interaction models are often convenient. Highly accurate theories of the free energy of the single-site exp-6 potential have been proposed [17–19]. In the current work, we use a numerical fit to free energies of the exp-6 fluid calculated from Ross's theory [18] and expressed as a polynomial in suitable variables [19,20]. The implementation of such theories is many orders of magnitude faster than particle-based simulations, thereby allowing for the rapid evaluation of thermodynamic properties at state points of interest. Since the equation of state used here becomes less accurate for subcritical conditions, the data for the exp-6 models at ambient pressure were obtained directly from isobaric–isothermal simulations of the liquid phase. Explicit simulations for the exp-6 models agree very well with the equation-of-state predictions at supercritical conditions.

The parameters for the single-site exp-6 models are listed in Table 1. The CH_4 model was simultaneously fit to experimental static compression data of Kortbeek et al. [21], as well as shock compression data of Nellis et al. [22]. Using the analytical equation of state in combination with a heat-capacity model, a reference single-site exp-6 interaction potential for CH_3OH was found by fitting to experimental sound speeds [23]. The model for O_2 was developed in a manner similar to the procedure used for CH_3OH. Sound speeds for O_2 at pressures up to 10 GPa have been reported by Abramson et al. [24]. The ammonia model was derived by fitting to the isotherms at 573–723 K reported by Harlow et al. [25].

3 Results and Discussion

Simulated and calculated densities for the TraPPE-UA force field and the single-site exp-6 models are compared to experimental data in Tables 2 and 3. The corresponding compressibility factors, $Z = pV_m/(RT)$, are plotted in Figs. 1 and 2.

For CH_4, both the TraPPE-UA and the exp-6 models match the experimental data [21] remarkably well at high temperature and pressure, but the exp-6 model shows a somewhat larger deviation for the liquid phase at ambient pressure. It appears that the nearly spherical and nonpolar CH_4 molecule can be well represented by single-site models over a wide range of state points. For NH_3, the 5-site TraPPE model always underpredicts the experimental high-temperature, high-pressure densities [25] (and overpredicts the compressibility factor), but falls within 4% of them. The exp-6 model, fit to these densities, matches even more closely, to within 2%. However, the

Table 2 Specific densities for CH_4 and NH_3

			Simulation		Equation of state	Experiment
			TraPPE-UA	exp-6	exp-6	
Molecule	T (K)	p (MPa)	ρ ($g \cdot cm^{-3}$)	ρ ($g \cdot cm^{-3}$)	ρ ($g \cdot cm^{-3}$)	ρ ($g \cdot cm^{-3}$)
CH_4	110	0.101	0.4232_5	0.4010_6		0.4248 [26]
	298	100	0.3416_1	0.3391_1	0.336	0.3411 [21]
	298	400	0.4719_1	0.4681_1	0.463	0.4721 [21]
	298	800	0.5433_1	0.5430_1	0.538	0.5437 [21]
	298	1,000	0.5677_1	0.5691_2	0.565	0.5688 [21]
	298	5,000	0.7731_9	0.8065_6		
	298	10,000	0.8686_7	0.9513_9		
NH_3	223	0.101	0.6978_3	0.6271_8		0.7023 [26]
	473	100	0.4672_1	0.4517_1	0.465	0.4928 [25]
	473	300	0.5941_5	0.6030_7	0.606	0.6218 [25]
	473	500	0.6550_1	0.6733_5	0.675	0.6846 [25]
	473	700	0.6970_2	0.7222_5	0.724	0.7259 [25]
	473	900	0.7298_1	0.7604_4	0.762	0.7560 [25]
	473	5,000	1.0211_2	1.0841_2		
	473	10,000	1.1432_3	1.2575_9		

Subscripts denote the standard deviation in the last digit for simulation data

Table 3 Specific densities and sound–speeds for O_2 and CH_3OH

			Simulation		Equation of state		Experiment	
			TraPPE-UA	exp-6	exp-6			
Molecule	T (K)	p (MPa)	ρ ($g \cdot cm^{-3}$)	ρ ($g \cdot cm^{-3}$)	ρ ($g \cdot cm^{-3}$)	c ($km \cdot s^{-2}$)	ρ ($g \cdot cm^{-3}$)	c ($km \cdot s^{-2}$)
O_2	80	0.101	1.1854_4	1.1157_6			1.1906 [26]	
	813	2890	1.5160_3	1.6091_1	1.600		3.0_1 [27]	
	813	2910	1.5189_5	1.6107_8	1.603		3.0_1 [27]	
	813	3060	1.5384_9	1.6337_9	1.626		3.1_1 [27]	
	813	3070	1.5395_4	1.6351_6	1.627		3.1_1 [27]	
	813	3870	1.6324_2	1.7434_4	1.734		3.17_5 [27]	
	813	7550	1.9130_9	2.0777_5	2.070		3.33_5 [27]	
	473	510	1.0608_1	1.0873_2				1.417 [24]
	473	1680	1.4516_2	1.5074_4				2.357 [24]
	473	3310	1.6912_5	1.7783_5				3.108 [24]
	473	5610	1.8907_4	2.0143_4				3.737 [24]
	473	7360	1.9986_2	2.1897_3				4.089 [24]
	473	10740	2.1556_7	2.3498_9				4.594 [24]
CH_3OH	298	0.101	0.7801_7	0.8935_7			0.7865 [26]	
	523	561	0.8845_3	1.0130_1	1.014	2.289		2.194 [23]
	523	987	0.9700_3	1.0925_8	1.094	2.719		2.720 [23]
	523	1424	1.0310_3	1.1520_7	1.154	3.058		3.000 [23]
	523	1633	1.0546_1	1.1754_8	1.178	3.197		3.219 [23]
	523	2640	1.1431_1	1.2765_7	1.272	3.751		3.771 [23]
	523	3160	1.1784_7	1.3115_9	1.310	3.986		4.023 [23]
	523	3890	1.2207_1	1.3499_7	1.357	4.278		4.255 [23]

Subscripts denote the standard deviation in the last digit for simulation data

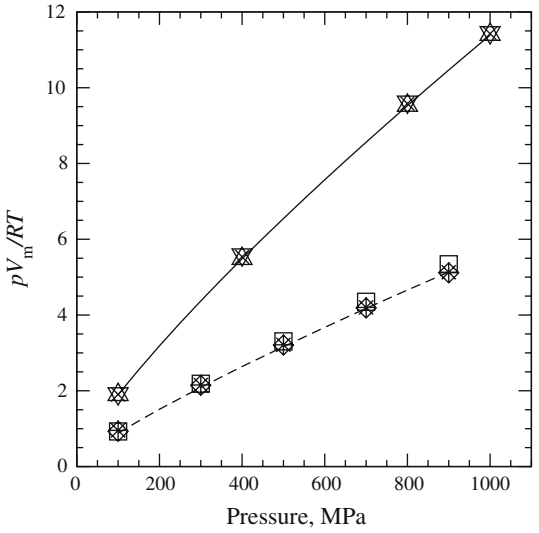

Fig. 1 Compressibility factors ($Z = PV_m/(RT)$) for CH_4 at 298 K (up triangles represent the TraPPE-UA model, down triangles represent the EOS predictions for the exp-6 model, and crosses represent the simulated exp-6 model) and NH_3 at 473 K (squares represent the TraPPE-UA model, diamonds represent the EOS predictions for the exp-6 model, and stars represent the simulated exp-6 model). Experimental data are depicted as a solid line for CH_4 and dashed line for NH_3

TraPPE model reproduces the ambient liquid-phase density [27], whereas the exp-6 model underpredicts it by about 10%. The simulations for the TraPPE-UA CH_4 and NH_3 models were also extended to very high pressures (5 and 10 GPa), which most likely fall into the meta-stable liquid region but nucleation of a solid phase was not observed.

Although there is fairly good agreement between the simulation data using the 3-site TraPPE model for O_2 and the equation of state data for the exp-6 model (with the TraPPE model yielding densities that are consistently lower by 6%), both models predict densities that fall about a factor of two below the experimental oxygen densities estimated by Johnson et al. [28] from the thermal decomposition of $KClO_3$ into KCl and O_2. The TraPPE model is able to match the ambient liquid-phase density of O_2 to within 1% while the exp-6 model somewhat underpredicts this density. Given the relatively good agreement between the two models and the fact that the exp-6 model was fitted to sound–speed measurements by Abramson et al. [24] and shown to be consistent with shock compression data [29] (see Fig. 3), it appears that the experimental densities reported by Johnson et al. [28] may not be accurate.

For CH_3OH, we were unable to find experimentally measured densities at high pressures and temperatures well-above the critical temperature. Thus, only an indirect comparison can be made to the the experimental sound speeds of Zaug et al. [23] which are well reproduced by the exp-6 model. The densities for the 3-site TraPPE-UA model fall roughly 12% below the densities obtained via the equation of state of the exp-6 model. It should be noted that a temperature of 523 K is rather close to the critical temperature. The 2% underestimation of the critical temperature by the

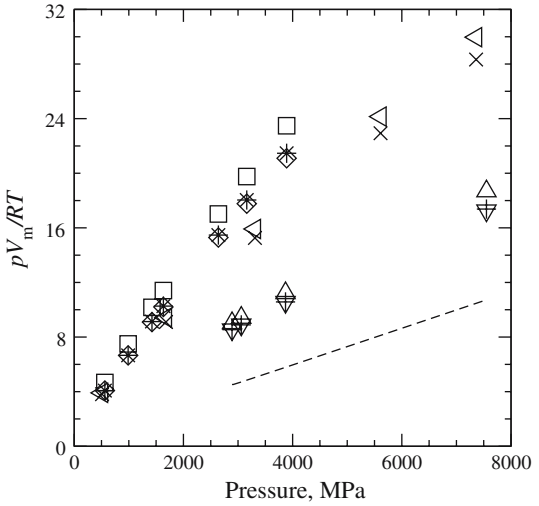

Fig. 2 Compressibility factors ($Z = PV_m/(RT)$) for O_2 at 813 K (up triangles represent the TraPPE-UA model, down triangles represent the EOS predictions for the exp-6 model, and +'s represent the simulated exp-6 model), O_2 at 473 K (left triangles represent the TraPPE-UA model and ×'s represent the simulated exp-6 model) and CH_3OH at 523 K (squares represent the TraPPE-UA model, diamonds represent the EOS predictions for the exp-6 model, and stars represent the simulated exp-6 model). Experimental compressibility factors are available only for O_2 at 813 K [28], and are shown with a dashed line

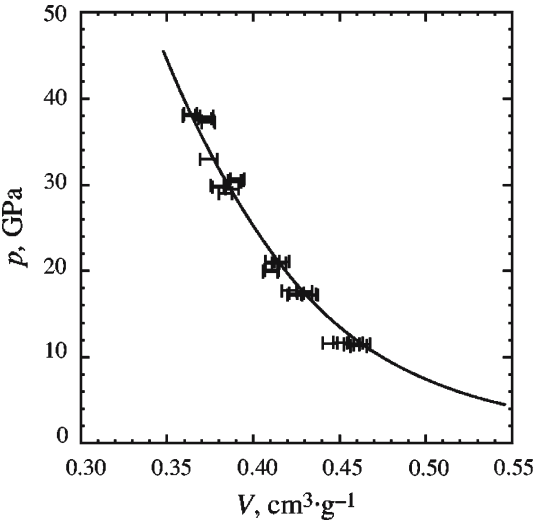

Fig. 3 The shock Hugoniot predicted with the single-site O_2 equation-of-state model compared with shock compression experiments. Calculated results are shown as a line, experimental results are shown as error bars

TraPPE CH_3OH model yields a reduced temperature of 1.04 at 523 K, whereas the correct value is 1.02. However, when both models are applied to state points at ambient pressure, the TraPPE model yields a liquid-phase density within 1% of experiment, while the exp-6 model overpredicts it by 14%.

Judging from these four examples, it appears that the TraPPE-UA model has a tendency to somewhat underpredict specific densities at high temperatures and pressures. Part of the discrepancy for the TraPPE densities can be attributed to the use of a LJ potential which is well-known to overestimate the repulsive interactions at high densities considered here (which are sometimes twice as high as the ambient liquid-phase densities used in TraPPE's parameterization).

4 Conclusions

The TraPPE force-field fitting philosophy dictates that parameters for a given interaction site should be the same, whether that site is in a different molecule or the system is at a different state point. While the fitting is done to vapor–liquid coexistence curves, the TraPPE model can be applied to other high-temperature, high-pressure state points with only a modest decrease in accuracy. Across all of the state points considered here, the TraPPE models reproduced the experimental densities at extreme conditions with an average error of 6%. The exp-6 models developed specifically for the experimental data studied here matched those values (not surprisingly) much more closely, with an error of about 2%. However, when the same models are applied to ambient pressure conditions, the TraPPE model reproduces experimental data with an average error of 1%, whereas the exp-6 models yield an average error of 9% at these conditions. When accurate experimental data at high pressures and temperatures are available, the fitting methodology of the exp-6 models allows data to be obtained with speed and accuracy. When experimental data are unavailable or available for only a limited range of state points, simulations using the TraPPE force field can provide reasonably accurate predictions and thereby supplement the sparse experimental data in the high-pressure/high-temperature regime.

Acknowledgments Financial support from the National Science Foundation (CTS-0553911 and ITR-0428774) is gratefully acknowledged. Part of this work was performed under the auspices of the US Department of Energy by the Lawrence Livermore National Laboratory under contract No. W-7405-ENG-48. Part of the computer resources were provided by the Minnesota Supercomputing Institute.

References

1. C. Cavazzoni, G.L. Chiarotti, S. Scandolo, E. Tosatti, M. Bernasconi, M. Parrinello, Science **283**, 44–46 (1999)
2. H.P. Scott, R.J. Hemley, H.-K. Mao, D.R. Herschbach, L.E. Fried, W.M. Howard, S. Bastea, Proc. Natl. Acad. Sci. **101**, 14023–14026 (2004)
3. M.G. Martin, J.I. Siepmann, J. Phys. Chem. B **102**, 2569–2577 (1998)
4. M.G. Martin, J.I. Siepmann, J. Phys. Chem. B **103**, 4508–4517 (1999)
5. C.D. Wick, M.G. Martin, J.I. Siepmann, J. Phys. Chem. B **104**, 8008–8016 (2000)
6. B. Chen, J.J. Potoff, J.I. Siepmann, J. Phys. Chem. B **105**, 3093–3104 (2001)

7. J.J. Potoff, J.I. Siepmann, AIChE J. **47**, 1676–1682 (2001)
8. J.M. Stubbs, J.J. Potoff, J.I. Siepmann, J. Phys. Chem. B **108**, 17596–17605 (2004)
9. Z.G. Zhang, Z.H. Duan, J. Chem. Phys. **122**, 214507-1–214507-15 (2005)
10. C.D. Wick, D.N. Theodorou, Macromolecules **37**, 7026–7033 (2004)
11. I.R. McDonald, Mol. Phys. **23**, 41–58 (1972)
12. J.P. Barker, R.O. Watts, Chem. Phys. Lett. **3**, 144–145 (1969)
13. J.I. Siepmann, D. Frenkel, Mol. Phys. **75**, 59–70 (1992)
14. L. Zhang, J.I. Siepmann, Theor. Chem. Acc. **115**, 391–397 (2006)
15. L. Zhang, J.I. Siepmann, Fluid Phase Equil. (In Preparation)
16. M.P. Allen, D.J. Tildesley, *Computer Simulation of Liquids* (Oxford University Press, Oxford, 1987)
17. M. Ross, J. Chem. Phys. **71**, 1567–1571 (1979)
18. H.S. Kang, C.S. Lee, T. Ree, F.H. Ree, J. Chem. Phys. **82**, 414–423 (1985)
19. L.E. Fried, W.M. Howard, J. Chem. Phys. **109**, 7338–7348 (1998)
20. W.B. Brown, J. Chem. Phys. **87**, 566–577 (1987)
21. P.J. Kortbeek, J.A. Schouten, Int. J. Thermophys. **11**, 455–466 (1990)
22. W.J. Nellis, F.H. Ree, M. van Thiel, A.C. Mitchell, J. Chem. Phys. **75**, 3055–3063 (1981)
23. J.M. Zaug, L.E. Fried, E.H. Abramson, D.W. Hansen, J.C. Crowhurst, W.M. Howard, High Pressure Res. **23**, 229–233 (2003)
24. Abramson, L.J. Slutsky, M.D. Harrell, J.M. Brown, J. Chem. Phys. **110**, 10493–10497 (1999)
25. Harlow, A., Wiegand, G., Franck, E.R.: Ber. Bunsenges. Phys. Chem. **101**, 1461–1465 (1997)
26. S.P. March, *LASL Shock Hugoniot Data* (University of California Press, Berkeley, California 1980)
27. E.W. Lemmon, M.O. McLinden, D.G. Friend, in *NIST Chemistry WebBook, NIST Standard Reference Database Number* 69, ed. by P.J. Linstrom, W.G. Mallard (National Institute of Standards and Technology, Gaithersburg, Maryland, 2005), http://www.webbook.nist.gov
28. M.C. Johnson, D. Walker, S.M. Clark, R.L. Jones, Am. Mineral. **86**, 1367–1379 (2001)
29. W.J. Nellis, A.C. Mitchell, J. Chem. Phys. **73**, 6137–6145 (1980)